Published OnlineFirst January 7, 2015; DOI: 10.1158/1535-7163.MCT-14-0710

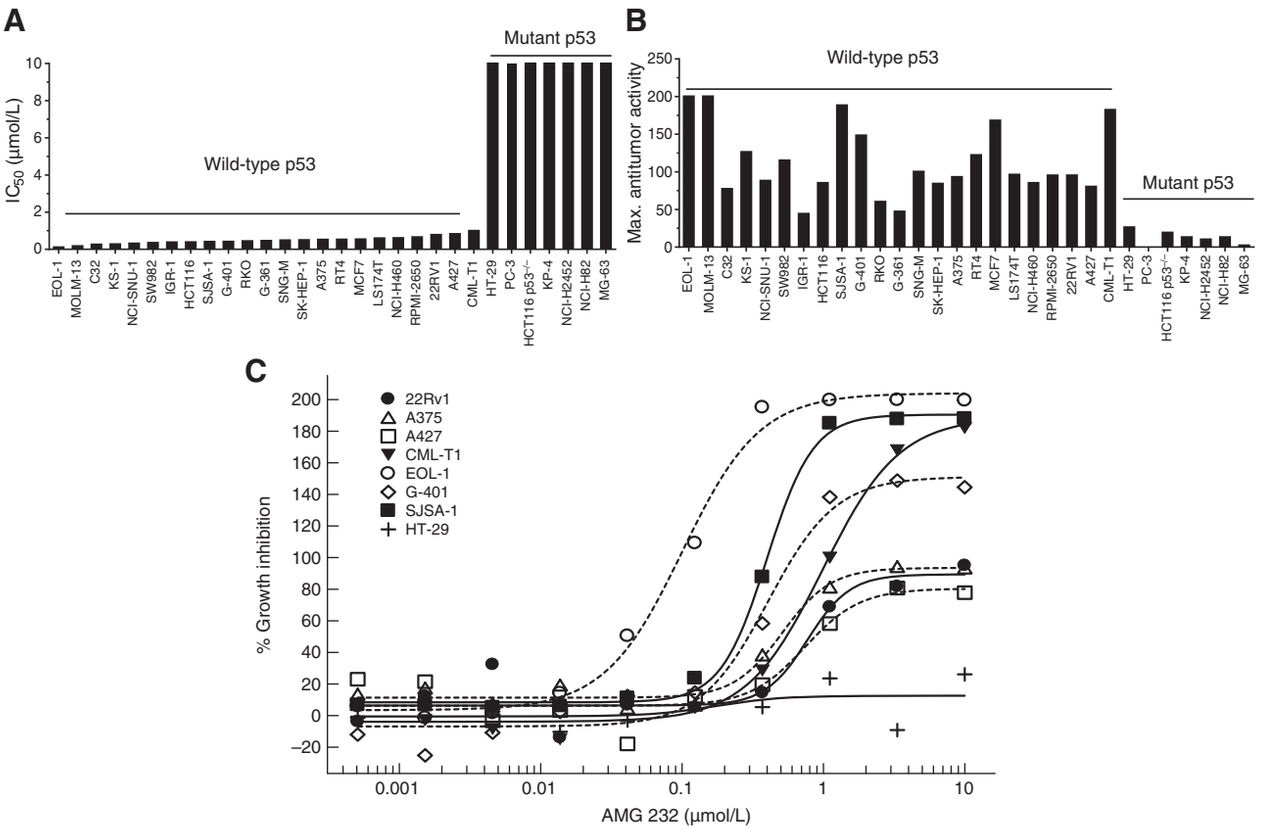

Figure 1.
AMG 232 inhibits cell proliferation in p53 WT cell lines *in vitro*. A, cell growth IC_{50} plot of 30 tumor cell lines treated with AMG 232 for 72 hours. B, maximum antitumor activity of AMG 232 treatment (10 μmol/L). 200% = complete cell killing, 100%, stasis; 0%, uninhibited cell growth (DMSO control). C, representative AMG 232 dose–response curves for a subset of the cell lines in A and B. Tumor cells were treated with DMSO control or AMG 232 (0.0005–10 μmol/L, 3-fold serial dilutions) for 72 hours. All cell lines shown in C are wild-type for p53, except HT-29, which is p53 mutant.

SJSA-1 and HCT116 tumors. Tumors treated with vehicle served as a negative control and indicated the baseline mRNA levels. AMG 232 treatment resulted in time- and dose-dependent induction of p21 mRNA in SJSA-1 tumors (Fig. 2B, top). p21 levels peaked at 4 hours after dose, and achieved maximal induction of approximately 30-fold over control in the 75 mg/kg group. In the 10 and 25 mg/kg groups, p21 levels were significantly elevated from 1 to 8 hours after dose, and returned to baseline levels by 24 hours. However, in the 75 mg/kg group, p21 levels remained significantly elevated out to 24 hours after dose. Similar effects were observed on MDM2 and PUMA expression in SJSA-1 tumors, where AMG 232 treatment caused a >10-fold induction of these p53 targets after 4 hours (75 mg/kg group; Fig. 2B, bottom), and sustained elevation out to 24 hours after dose. AMG 232 treatment also caused a dose-dependent induction of p21, MDM2, and PUMA mRNA in HCT116 tumors (Fig. 2C). At 6 hours after dose, AMG 232 treatment of HCT116 tumor-bearing mice caused induction of p21 and MDM2 transcript levels by approximately 13-fold and approximately 4-fold over control (100 and 15 mg/kg, respectively). PUMA expression was also significantly elevated in HCT116 tumors, but the magnitude of PUMA induction (4-fold in 100 mg/kg group) was less than the other p53 targets, and less than PUMA induction observed in SJSA-1 tumors. For an additional pharmacodynamic readout of p53 pathway activity, we measured the secreted protein MIC-1 (human specific) in the plasma of AMG 232-treated, HCT116 tumor-bearing mice. MIC-1 protein was elevated by 6-fold (100 mg/kg) and 3-fold (15 mg/kg) after 6 hours of AMG 232 treatment (Fig. 2D). Taken together, the induction of p21, MDM2, PUMA, and MIC-1 indicated on-mechanism activation of the p53 pathway by AMG 232 treatment.

AMG 232 potently inhibits growth of tumor xenografts in mice

We evaluated the antitumor activity of AMG 232 in xenograft models representing different genetic backgrounds and various tumor types. All tumor cell lines utilized in xenograft models harbored wild-type p53. Daily oral administration of AMG 232 resulted in significant tumor growth inhibition (TGI) across all models (Fig. 3A, C, E, and G). SJSA-1, an MDM2 amplified osteosarcoma model, was the most sensitive to AMG 232 treatment with an ED_{50} of 9.1 mg/kg. In the highest dose group of 75 mg/kg, 10 of 10 tumors completely regressed and were undetectable after 10 days of treatment. AMG 232 treatment was stopped in this group after day 25, and mice were observed for an additional 50 days. There was no detectable SJSA-1 tumor regrowth in any of the mice. Additional xenograft

Published OnlineFirst January 7, 2015; DOI: 10.1158/1535-7163.MCT-14-0710

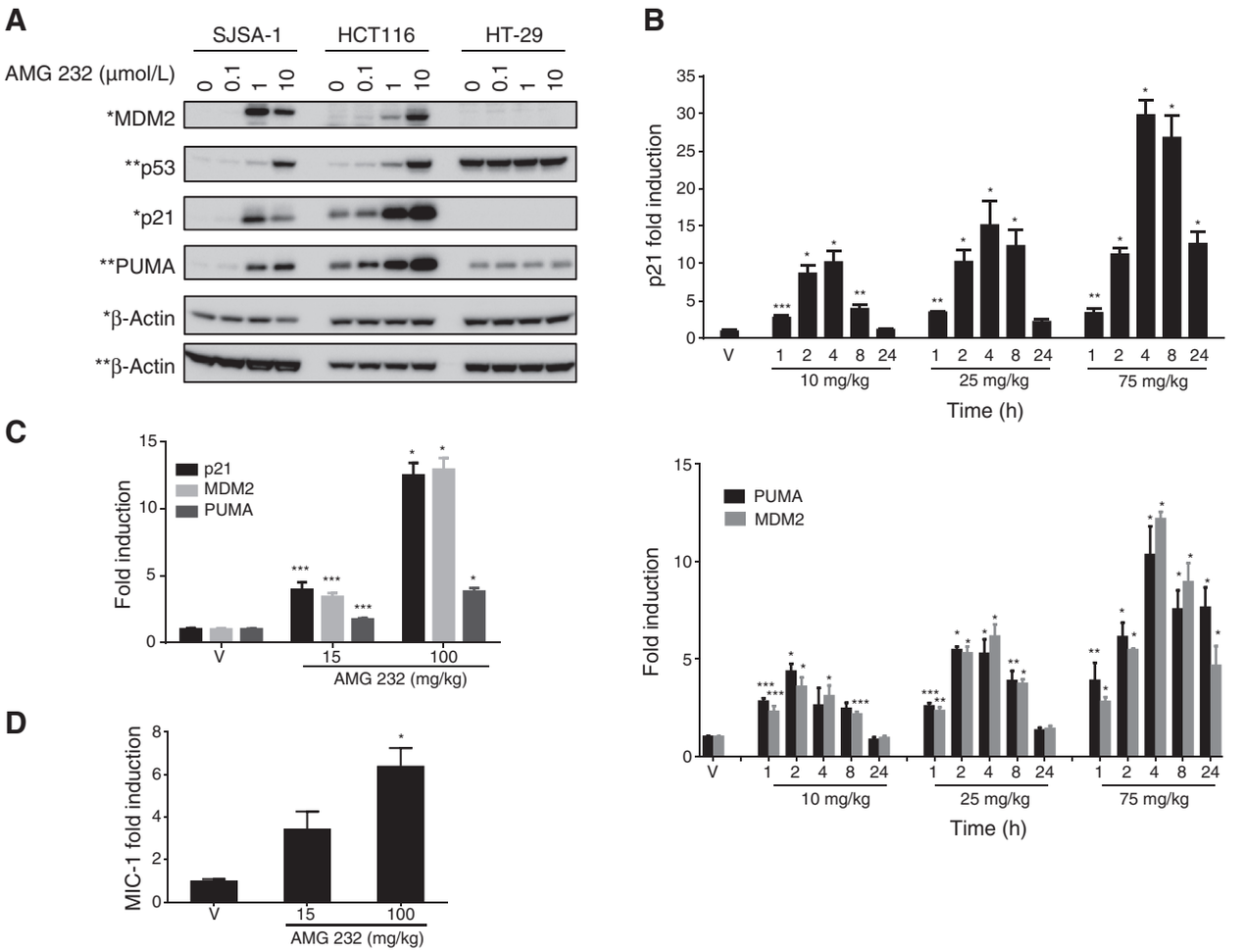

Figure 2.
AMG 232 treatment induces p53 pathway activity *in vitro* and *in vivo*. A, AMG 232 leads to increased p53, p21, MDM2, and PUMA proteins in p53 wild-type cells (SJSA-1, HCT116) but not in p53-mutant HT-29 cells. Because of very high induction of p21 and MDM2 proteins in SJSA-1 cells, reduced protein was loaded (*, 2 μg protein/lane SJSA-1, 20 μg/lane HCT116 and HT-29; **, 20 μg protein/lane all). B, AMG 232 induces p21 (top), MDM2, and PUMA mRNA (bottom) in SJSA-1 tumor cells *in vivo* in a time- and dose-dependent manner. Mice were treated with one dose of AMG 232, and tumors were harvested at the indicated time points and analyzed for transcript levels. C and D, AMG 232 induces p21, MDM2, PUMA, and MIC-1 in HCT116 tumor cells *in vivo*. Mice were treated with AMG 232 once daily for 2 days, and tumors (C) or serum (D) were harvested for analysis 6 hours after the last dose. Data, mean fold increase over vehicle-treated controls ± SEM. $n = 4$/group. *, $P < 0.0001$; **, $P < 0.001$; ***, $P < 0.05$.

models demonstrated a range of *in vivo* antitumor activity of AMG 232. In the HCT116 colorectal cancer model (*KRAS* mutant), the highest dose of AMG 232 resulted in 86% TGI compared with control, and the ED_{50} was 31 mg/kg (Fig. 3C). AMG 232 treatment in an A375sq2 *BRAF*-mutant melanoma model resulted in 97% TGI, with an ED_{50} of 18 mg/kg (Fig. 3E). The NCI-H460 non–small cell lung cancer model was the least sensitive, where AMG 232 treatment resulted in 60% TGI at the highest dose, with an ED_{50} of 78 mg/kg (Fig. 3G). There was no body weight loss in any of the AMG 232 xenograft studies (Supplementary Fig. S3). To note, AMG 232 displays approximately 40-fold less biochemical potency on murine MDM2 compared with human MDM2 (data not shown).

Tumors were harvested at the end of each xenograft study to determine the effect of AMG 232 treatment on p53 pathway activity. AMG 232 treatment resulted in a dose- and time-dependent induction of p21 mRNA compared with vehicle-treated tumors (Fig. 3B, D, F, and H). The level of p21 induction within each tumor model related to the degree of TGI, where p21 levels were highest in tumors whose growth was most inhibited. However, the maximum p21 induction level varied across tumor models.

AMG 232 blocks DNA synthesis and induces apoptosis *in vivo*

To further understand the mechanism whereby AMG 232 caused inhibition of tumor growth *in vivo*, we assessed the effect of AMG 232 treatment on cell cycle and apoptosis. Incorporation of BrdUrd and cleavage of caspase-3 were examined by IHC in the SJSA-1 and HCT116 xenografts, representing, respectively, a model that regresses and a model that undergoes cytostasis after AMG 232 treatment (Fig. 3A and C). Tumor-

Published OnlineFirst January 7, 2015; DOI: 10.1158/1535-7163.MCT-14-0710

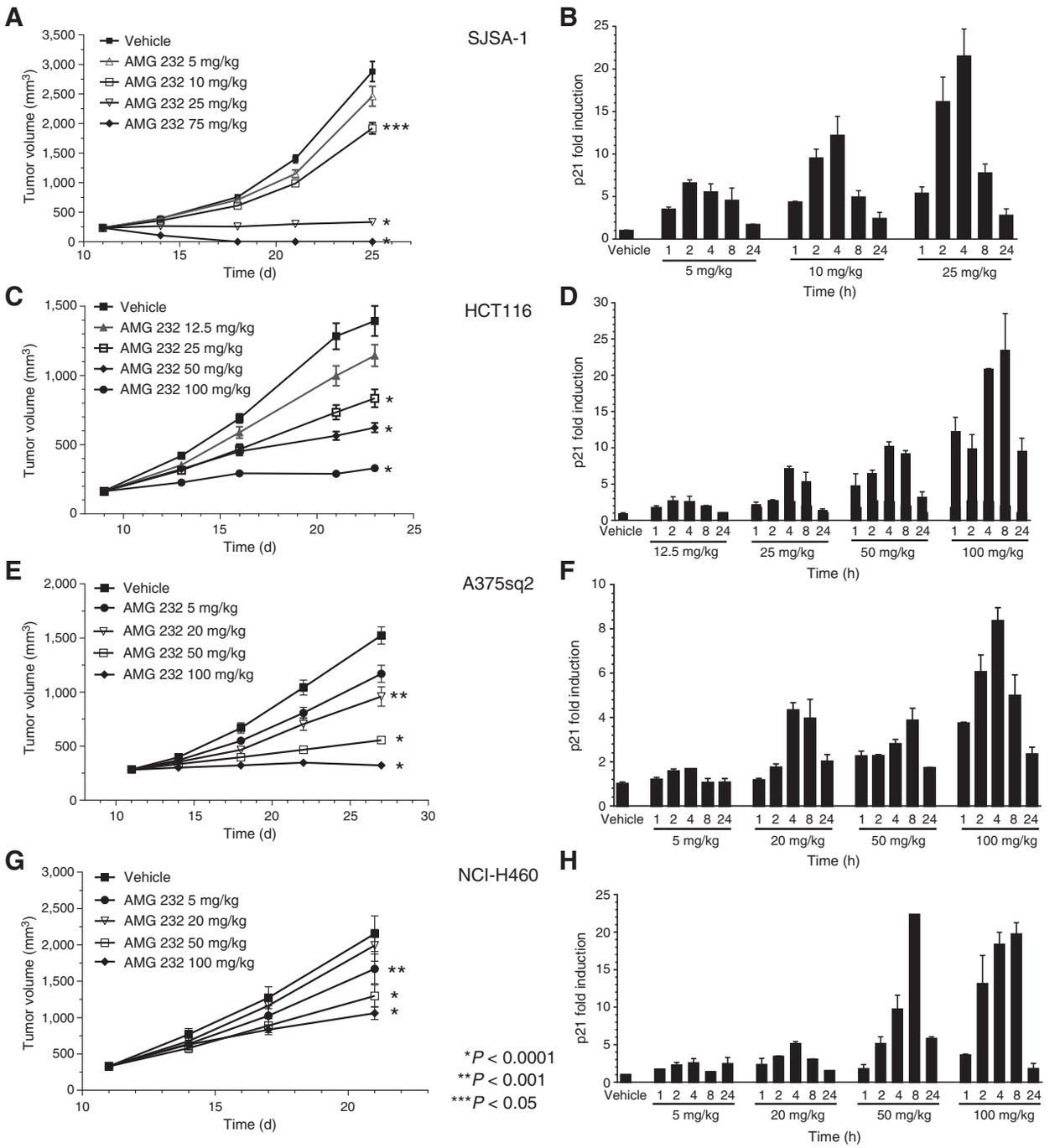

Figure 3.
AMG 232 treatment inhibits tumor growth *in vivo* in a broad range of tumor models. For each xenograft model, the left panel shows the effect of AMG 232 treatment on tumor growth over time ($n = 10$/group), and the right panel is the effect on p21 mRNA induction in tumors taken at the end of the study (at 1, 2, 4, 8, or 24 hours. $n = 2$/time point). Treatment began when tumors reached approximately 200 mm^3, and all groups were treated daily by oral gavage. Data, mean ± SEM. *, $P < 0.0001$; **, $P < 0.001$; ***, $P < 0.05$ compared with vehicle control group. A and B, SJSA-1. C and D, HCT116. E and F, A375sq2. G and H, NCI-H460.

bearing mice were treated daily with AMG 232 or vehicle control, and tumors were harvested 6 hours after one dose (day 1) or four doses (day 4). In the SJSA-1 tumors, there was a significant decrease in BrdUrd incorporation after one dose, and a marked decrease (88%) after 4 days of dosing (Fig. 4A and B), demonstrating a robust inhibition of the cell cycle by AMG 232. Concomitantly, increased cleaved caspase-3 staining was observed after one dose, which was further increased by day 4 when a marked 12-fold induction of cleaved caspase-3 was observed (Fig. 4C and D). In HCT116 tumors, there was no

Published OnlineFirst January 7, 2015; DOI: 10.1158/1535-7163.MCT-14-0710

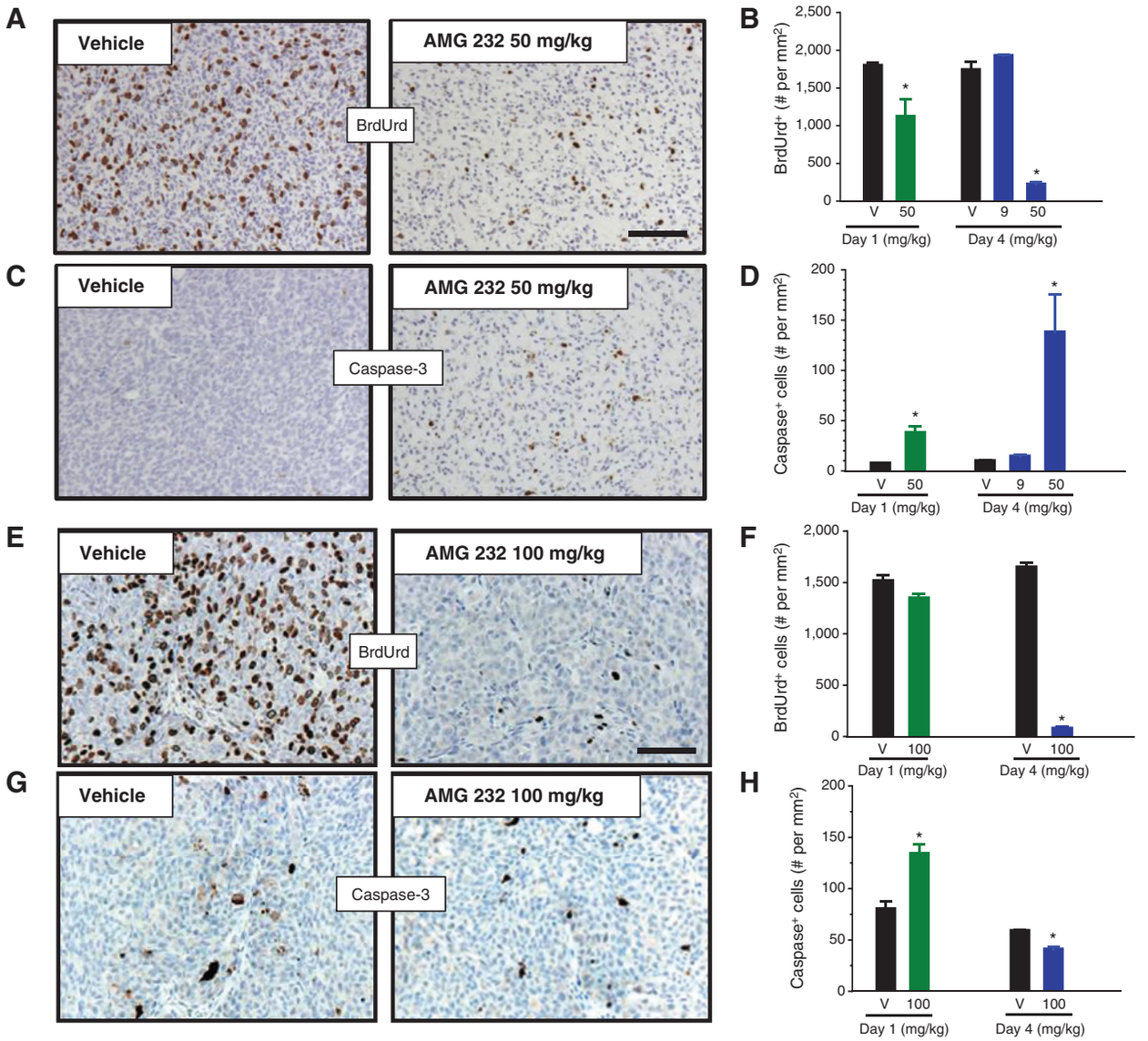

Figure 4.

AMG 232 treatment causes cell-cycle arrest and induces apoptosis *in vivo*. Mice bearing SJSA-1 (A–D) or HCT116 (E–H) tumors were treated with vehicle control or AMG 232 for 4 days. Tumors were harvested 6 hours after treatment on days 1 and 4, fixed, and processed for IHC detection of BrdUrd (A and E) and cleaved caspase-3 (C and G). Representative images of each group are shown from day 4. Bars, 100 μm. B, D, F and H, quantification of the BrdUrd and cleaved caspase-3 staining from each group ($n = 10$/group). Data, mean ± SEM. *, $P < 0.005$.

detectable effect on the cell cycle after one dose (6 hours); however, by day 4, AMG 232 treatment caused a 96% decrease in BrdUrd incorporation (Fig. 4E and F). There was a moderate increase in cleaved caspase-3 staining in HCT116 tumors after one dose, but this effect reversed and after 4 days of AMG 232 treatment cleaved caspase-3 levels were slightly less than control tumors (Fig. 4G and H). Taken together, AMG 232 treatment resulted in marked reductions in BrdUrd incorporation in both tumor models, reflecting a robust arrest of the cell cycle. Apoptosis was induced more dramatically in the SJSA-1 tumor model compared with HCT116, consistent with the observations of tumor regression and cytostasis, respectively, after AMG 232 treatment (Fig. 3A and B).

AMG 232 potentiates the antitumor activity of p53-inducing cytotoxics *in vivo*

We investigated combination treatment of AMG 232 with several standards of care where there was clear biologic rationale to support an interaction in the p53 pathway. Cytotoxic agents that induce DNA damage and p53 activation were evaluated in relevant tumor models. We first tested the combination of AMG 232 with platinum-containing agents in the non–small cell lung cancer model NCI-H460, which is moderately resistant to AMG 232 treatment alone (Fig. 3G). AMG 232 was dosed at its maximally effective dose (100 mg/kg) in this model and was combined with the MTD of cisplatin (5 mg/kg) in mice. Although both agents inhibited tumor

Published OnlineFirst January 7, 2015; DOI: 10.1158/1535-7163.MCT-14-0710

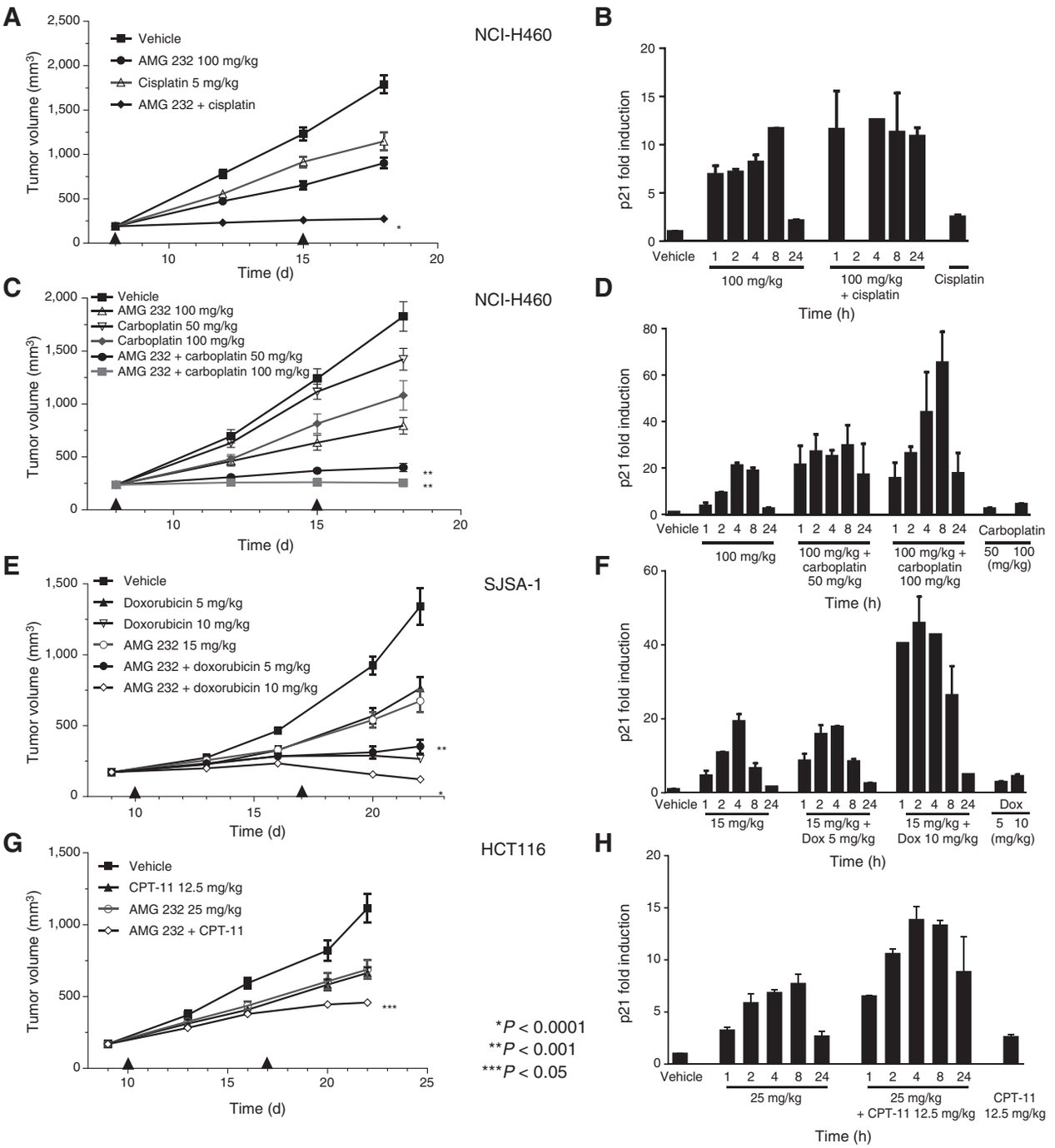

Figure 5.
AMG 232 enhances the antitumor activity of DNA-damaging cytotoxics. AMG 232 or vehicle control was dosed orally once daily in combination with cisplatin (A), carboplatin (C), doxorubicin (E), or CPT-11 (G), which were dosed once weekly (indicated by arrowheads on *x*-axes). Data, mean tumor volume ± SEM ($n = 10$/group). *, $P < 0.0001$; **, $P < 0.005$; ***, $P < 0.05$. *P* values are for comparisons of the combination treatment to each single agent in that combination. B, D, F, H, quantification of p21 mRNA induction in tumors harvested at the end of the xenograft studies. $n = 2$/time point at 1, 2, 4, 8, and 24 hours after last treatment of AMG 232. In B, there was insufficient RNA recovered at the 2-hour time point from the combination group. For p21 analysis in the cytotoxic treatments alone, tumor harvest was 4 days (cisplatin, carboplatin) or 6 days (doxorubicin, CPT-11) after last dose of chemo.

growth compared with vehicle control, the combination treatment resulted in synergistic antitumor efficacy and caused tumor stasis (Fig. 5A). Similarly, we combined AMG 232 (100 mg/kg) with carboplatin at two different doses (50 and 100 mg/kg). In each case, the combination of AMG 232 with carboplatin resulted in superior antitumor efficacy (Fig. 5C).

Published OnlineFirst January 7, 2015; DOI: 10.1158/1535-7163.MCT-14-0710

Notably, the combination with the lower dose of carboplatin (50 mg/kg) resulted in similar antitumor efficacy compared with the combination with the higher dose of carboplatin (100 mg/kg), consistent with a synergistic effect. To determine the effect of combination treatment on p53 pathway activity, tumors were harvested at the end of the studies for p21 analysis. In the AMG 232-cisplatin study, AMG 232 alone induced p21 over time, and p21 levels returned to baseline by 24 hours (Fig. 5B). Cisplatin alone induced p21 minimally (2.5-fold). However, in the AMG 232–cisplatin combination, p21 levels were elevated more than 10-fold, which was sustained across the full 24 hours. Similarly, in the AMG 232–carboplatin combination study, the amplitude and duration of p21 induction in the combination treatments were markedly higher than either of the single-agent treatments (Fig. 5D), with a peak of >60-fold induction of p21 in the higher dose combination group. Of note, the last cisplatin and carboplatin doses were administered 4 days before the end of the study and tumor harvest, indicating a prolonged and sustained combination effect on p53 pathway activation.

We tested the combination of AMG 232 with doxorubicin in the SJSA-1 sarcoma model. The SJSA-1 model is sensitive to AMG 232 treatment alone (Fig. 3A), therefore a suboptimal dose (15 mg/kg) of AMG 232 was used for this combination. As single agents, both dose levels of doxorubicin and AMG 232 alone inhibited tumor growth compared with the control group (Fig. 5E). In combination, AMG 232 plus doxorubicin resulted in superior antitumor efficacy, with the higher dose combination (doxorubicin 10 mg/kg) resulting in tumor regression. Induction of p21 by doxorubicin treatment alone (10 mg/kg) was approximately 5-fold. AMG 232 treatment alone resulted in peak p21 induction of approximately 20-fold. However, p21 levels were elevated approximately 40-fold in the higher dose combination treatment group (Fig. 5F), indicating that p53 pathway activation was highest in tumors that regressed. Furthermore, the increased p21 induction in this combination group was prolonged 6 days after the final dose of doxorubicin.

We also evaluated the combination of AMG 232 with irinotecan (aka, CPT-11) in the HCT116 colorectal carcinoma model. The combination treatment resulted in significantly improved antitumor efficacy compared with the single agents (Fig. 5G). Similarly, p21 levels were induced higher and for a longer duration after combination treatment (Fig. 5H) compared with the single-agent treatments. There was no significant body weight loss in any of the combination studies (Supplementary Fig. S3).

Discussion

Herein, we have characterized the *in vitro* and *in vivo* attributes of AMG 232, the most potent MDM2 inhibitor described to date. AMG 232 binds to MDM2 with picomolar affinity (K_D 0.045 nmol/L) and inhibits the MDM2–p53 interaction in a biochemical cell-free assay with an IC_{50} of 0.6 nmol/L. Treatment of tumor cells with AMG 232 *in vitro* resulted in robust activation of the p53 pathway leading to inhibition of proliferation. Tumor cells underwent growth arrest, and this was related to induction of p21, a direct transcriptional target of p53 and a mediator of cell-cycle arrest. AMG 232 treatment also resulted in stabilization of p53 protein and increased levels of MDM2, p21, and PUMA proteins in p53 wild-type cells. In a broad panel of tumor cell lines, AMG 232 treatment inhibited the growth of p53 wild-type cells in a 3-day viability assay, whereas there was no significant effect on p53-mutant tumor cells (Fig. 1A). This suggests that the antiproliferative response to AMG 232 is dependent on p53. However, we did not investigate the possible role of other p53 family members (e.g., p73) in this study. The maximum antitumor effect of AMG 232 treatment varied across the p53 wild-type cells with some cell lines undergoing complete cell killing whereas others were cytostatic (Fig. 1B). This observation is consistent with other reports, suggesting that the propensity of tumor cells to undergo apoptosis after MDM2 inhibition varies across cell lines (9).

Pharmacodynamic assays revealed that AMG 232 caused potent activation of p53 signaling *in vivo*. The exceptional *in vivo* properties of AMG 232 led to significant induction of p21, MDM2, and PUMA expression for 24 hours after a single dose (Fig. 2B). Induction of p21 occurred in SJSA-1 cells, which undergo complete cell killing *in vitro*, as well as in HCT116 cells that reflect a growth-arrest phenotype. This suggests that cell-cycle arrest via p21 activity occurs as an initial response to MDM2 inhibition independent of the ultimate outcome of inhibition of proliferation and/or apoptosis. PUMA induction was more pronounced in SJSA-1 tumors compared with HCT116 tumors, consistent with their apoptotic versus growth-arrest phenotypes, respectively.

AMG 232 demonstrated antitumor activity *in vivo* in a variety of tumor types with different genetic backgrounds. The MDM2-amplified SJSA-1 model was the most sensitive to AMG 232 treatment, which caused complete tumor regression and no evidence of tumor regrowth after cessation of treatment. AMG 232 was also effective at inhibiting tumor growth in models that harbor mutations in MAPK signaling pathways (e.g., *KRAS*-mutant HCT116 and *BRAF*-mutant A375), indicating that restoration of p53 tumor-suppressive function is broadly effective in tumors that are p53 wild-type. Tumor regression was not observed in all models, indicating that some tumor cells are more resistant to undergoing apoptosis after MDM2 inhibition. *In vivo* mechanism of action studies assessing cell-cycle progression (BrdUrd) and cell death (cleaved caspase-3) demonstrated that AMG 232 induced rapid cell-cycle arrest in both SJSA-1 and HCT116 tumors, but marked induction of apoptosis was observed only in the SJSA-1 line.

Given the high genetic diversity of tumors and frequent emergence of resistance to targeted and cytoxic agents in the clinic, MDM2 inhibitors will likely be combined with other therapies to achieve better clinical responses. To that end, we evaluated combination treatment with several cytotoxic agents where there was mechanistic rationale for an antitumor interaction with MDM2 inhibition. Cisplatin and carboplatin are platinum-based chemotherapeutics that bind and cross-link DNA, causing inhibition of DNA repair and synthesis (16). They are standards of care for various cancers, including lung and ovarian carcinomas. Doxorubicin is an anthracycline that intercalates DNA and blocks the progression of topoisomerase-2, inhibiting DNA replication (17). It is used to treat a wide range of cancers, including hematologic malignancies and sarcomas. Irinotecan (aka CPT-11) is a topoisomerase-1 inhibitor and leads to DNA fragmentation and inhibition of replication, and is primarily used to treat colorectal carcinomas (17). The mechanism of tumor cell death by DNA-damaging cytotoxic drugs like these is largely mediated by induction of

Published OnlineFirst January 7, 2015; DOI: 10.1158/1535-7163.MCT-14-0710

the p53 pathway (18), which leads to growth arrest and apoptosis. However, the full tumor-killing potential of such agents may be limited by insufficient p53 activity in tumor cells that may have faulty cell-cycle checkpoint controls. We hypothesized that combining MDM2 inhibition with such agents may restore the full tumor-suppressive function of p53 and increase antitumor efficacy. We tested this hypothesis by combining AMG 232 with these agents in relevant tumor models. In each case, the addition of MDM2 inhibition by AMG 232 to chemotherapy treatment led to significantly improved antitumor efficacy, and this was related to a marked increase in p53 signaling as evidenced by dramatic and sustained induction of p21 in the combination treatment groups lasting 4 to 6 days after the last doses of chemotherapies.

The data presented here support the investigation of AMG 232 treatment alone, and in combination with standard-of-care agents, in patients with cancer. AMG 232 is currently being evaluated in clinical trials.

Disclosure of Potential Conflicts of Interest

J.D. Oliner has immediate family members with ownership interest (including patents) in Amgen. A. Coxon has ownership interest in Amgen Inc. stock. No potential conflicts of interest were disclosed by the other authors.

Authors' Contributions

Conception and design: J. Canon, S.H. Olson, Q. Ye, L. Jin, S. Kaufman, R. Kendall, J.D. Oliner, A. Coxon, R. Radinsky

Development of methodology: J. Canon, T. Osgood, A.Y. Saiki, R. Robertson, D. Yu, J. Zhou, S. Kaufman

Acquisition of data (provided animals, acquired and managed patients, provided facilities, etc.): J. Canon, T. Osgood, S.H. Olson, A.Y. Saiki, R. Robertson, D. Yu, A. Chen, D. Cordover, S. Kaufman

Analysis and interpretation of data (e.g., statistical analysis, biostatistics, computational analysis): J. Canon, T. Osgood, A.Y. Saiki, R. Robertson, D. Yu, J. Eksterowicz, Q. Ye, J. Zhou, D. Cordover, S. Kaufman, J.D. Oliner, A. Coxon, R. Radinsky

Writing, review, and/or revision of the manuscript: J. Canon, T. Osgood, S.H. Olson, Q. Ye, S. Kaufman, R. Kendall, J.D. Oliner, A. Coxon, R. Radinsky

Administrative, technical, or material support (i.e., reporting or organizing data, constructing databases): T. Osgood, R. Robertson, Q. Ye, S. Kaufman

Study supervision: J. Canon, T. Osgood, R. Radinsky

Acknowledgments

The authors thank Annie Luo, Darlene Kratavil, Chris De La Torre, Gwyneth Van, and Efrain Pacheco for IHC and histology support.

The costs of publication of this article were defrayed in part by the payment of page charges. This article must therefore be hereby marked *advertisement* in accordance with 18 U.S.C. Section 1734 solely to indicate this fact.

Received August 25, 2014; revised December 18, 2014; accepted December 22, 2014; published OnlineFirst January 7, 2015.

References

1. Vogelstein B, Lane D, Levine AJ. Surfing the p53 network. Nature 2000; 408:307–10.
2. Vazquez A, Bond EE, Levine AJ, Bond GL. The genetics of the p53 pathway, apoptosis and cancer therapy. Nat Rev Drug Discov 2008;7:979–87.
3. Olivier M, Hollstein M, Hainaut P. TP53 mutations in human cancers: origins, consequences, and clinical use. Cold Spring Harb Perspect Biol 2010;2:a001008.
4. Chene P. Inhibiting the p53-MDM2 interaction: an important target for cancer therapy. Nat Rev Cancer 2003;3:102–9.
5. Harris SL, Levine AJ. The p53 pathway: positive and negative feedback loops. Oncogene 2005;24:2899–908.
6. Oliner JD, Pietenpol JA, Thiagalingam S, Gyuris J, Kinzler KW, Vogelstein B. Oncoprotein MDM2 conceals the activation domain of tumour suppressor p53. Nature 1993;362:857–60.
7. Vassilev LT, Vu BT, Graves B, Carvajal D, Podlaski F, Filipovic Z, et al. *In vivo* activation of the p53 pathway by small-molecule antagonists of MDM2. Science 2004;303:844–8.
8. Mohammad RM, Wu J, Azmi AS, Aboukameel A, Sosin A, Wu S, et al. An MDM2 antagonist (MI-319) restores p53 functions and increases the life span of orally treated follicular lymphoma bearing animals. Mol Cancer 2009;8:115.
9. Tovar C, Graves B, Packman K, Filipovic Z, Higgins B, Xia M, et al. MDM2 small-molecule antagonist RG7112 activates p53 signaling and regresses human tumors in preclinical cancer models. Cancer Res 2013;73:2587–97.
10. Rew Y, Sun D, Gonzalez-Lopez De Turiso F, Bartberger MD, Beck HP, Canon J, et al. Structure-based design of novel inhibitors of the MDM2-p53 interaction. J Med Chem 2012;55:4936–54.
11. Ding Q, Zhang Z, Liu JJ, Jiang N, Zhang J, Ross TM, et al. Discovery of RG7388, a potent and selective p53-MDM2 inhibitor in clinical development. J Med Chem 2013;56:5979–83.
12. Sun D, Li Z, Rew Y, Gribble M, Bartberger MD, Beck HP, et al. Discovery of AMG 232, a potent, selective, and orally bioavailable MDM2-p53 inhibitor in clinical development. J Med Chem 2014;57: 1454–72.
13. Carnahan J, Beltran PJ, Babij C, Le Q, Rose MJ, Vonderfecht S, et al. Selective and potent Raf inhibitors paradoxically stimulate normal cell proliferation and tumor growth. Mol Cancer Ther 2010;9:2399–410.
14. Carry JC, Garcia-Echeverria C. Inhibitors of the p53/hdm2 protein-protein interaction-path to the clinic. Bioorg Med Chem Lett 2013;23: 2480–5.
15. Masuya K, Furet P, Stutz S, Holzer P, Pissot-Soldmann C, Buschmann N, et al.Discovery of CGM097 as a novel Mdm2 inhibitor[abstract]. In: Proceedings of the 105th Annual Meeting of the American Association for Cancer Research; 2014 Dec 5–9; San Diego, CA. Abstract nr DDT01-01.
16. Poklar N, Pilch DS, Lippard SJ, Redding EA, Dunham SU, Breslauer KJ. Influence of cisplatin intrastrand crosslinking on the conformation, thermal stability, and energetics of a 20-mer DNA duplex. Proc Natl Acad Sci U S A 1996;93:7606–11.
17. Pommier Y, Leo E, Zhang H, Marchand C. DNA topoisomerases and their poisoning by anticancer and antibacterial drugs. Chem Biol 2012; 17:421–33.
18. Lakin ND, Jackson SP. Regulation of p53 in response to DNA damage. Oncogene 1999;18:7644–55.